Robotica (2019) volume 37, pp. 1033–1056. © Cambridge University Press 2019
doi:10.1017/S026357471800142X

Robust Output-Feedback Formation Control Design for Nonholonomic Mobile Robot (NMRs)

Bilal M. Yousuf*

Department of Electronics and Power Engineering, Pakistan Navy Engineering College, National University of Sciences and Technology (NUST), Karachi, Pakistan

(Accepted December 5, 2018. First published online: January 31, 2019)

SUMMARY

This paper addresses the systematic approach to design formation control for kinematic model of unicycle-type nonholonomic mobile robots. These robots are difficult to stabilize and control due to their nonintegrable constraints. The difficulty of control increases when there is a requirement to control a cluster of nonholonomic mobile robots in specific formation. In this paper, the design of the control scheme is presented in a three-step process. First, a robust state-feedback point-to-point stabilization control is designed using sliding mode control. In the second step, the controller is modified so as to address the tracking problem for time-varying reference trajectories. The proposed control scheme is shown to provide the desired robustness properties in the presence of the parameter variation, in the region of interest. Finally, in third step, tracking problem of a single nonholonomic mobile robot extends to formation control for a group of mobile robots in the leader–follower scenario using integral terminal- based sliding mode control augmented with stabilizing control. Starting with the transformation of the mathematical model of robots, the proposed controller ensures that the robots maintain a constant distance between each other to avoid collision. The main problem with the proposed controller is that it requires all states specially velocities. Therefore, the state-feedback control scheme is then extended to output feedback by incorporating a highgain observer. With the help of Lyapunov analysis and appropriate simulations, it is shown that the proposed output-feedback control scheme achieves the required control objectives. Furthermore, the closed loop system trajectories reach to desired equilibrium point in finite time while maintaining the special pattern.

KEYWORDS: Nonholonomic mobile robots; Robust control; Integral terminal sliding mode control; Stabilization; Tracking; Formation control; Graph theory; High-gain observer; Lyapunov analysis.

1. Introduction

Over the past decade, a number of researchers have contributed toward the analysis and control design of under-actuated and nonholonomic robotic systems. The motivation and interest have been primarily sparked by the fact that such under-actuated and nonholonomic systems present some very interesting, yet challenging, control problems which arise in a variety of practical applications, such as robotics, control of autonomous vehicles as well as electromechanical systems for which the number of actuators is smaller than the number of degrees of freedom. In today's world, Wheeled Mobile Robots (WMRs) are increasingly finding their presence and utilization in industrial as well as service enterprises, particularly with respect to their capability of an accurate autonomous motion (e.g., stabilization as well as tracking) while achieving the desired degree of obstacle avoidance, etc. WMRs are known to be nonholonomic, that is, they are subject to some of the nonholonomic

* Corresponding author. E-mail: bilalmyousuf4@gmail.com

constraints that arise in control of a WMR due to their nonintegrable properties. The multi-robot system exhibits more expensive but a better solution for specific tasks, which cannot be managed by a single robot. A multi-robotic system is used for a variety of applications like rescue operations mapping of an unknown and dangerous environment, etc. In leader–follower formation control, the leader solves the problem of planning and navigation, and the followers just follow the leader while performing their own task. In this paper, we focus our attention on designing of a nonlinear controller that achieves formation control objectives for a group of nonholonomic wheeled mobile robot (NMRs).

In control theory, trajectory tracking and formation are important as well as a challenging problem, especially when the system is exposed to unknown disturbances/parametric variations, etc. Several researchers have contributed to the solution of this problem, thereby proposing various techniques and solutions. Gao and Shang, in ref. [1], have addressed the state-feedback stabilization problem for a mobile robot by transforming the system into a normal form using input-state scaling along with a back-stepping recursive approach. Lee et al., in ref. [2], presented the unique idea of using the Radio Frequency Identification (RFID) sensor to estimate the real posture of NMR. The scheme uses sliding mode control for the tracking NMR to desired trajectories. Lefeber et al., in ref. [3], have suggested the control law based on the adaptive control scheme. They used an adaptation method to make the system more robust as compared to other algorithms. Peng et al., in ref. [4], have presented the formation control for NMR utilizing the leader–follower scenario. The design of the control scheme is based on second-order adaptive control augmented with a bioinspired neurodynamic approach. They introduced a novel method based on input constraints. Dong et al., in ref. [5], have proposed formation control based on the distributed technique for nonholonomic mobile robots. This approach was proposed with the aid of cascaded systems, such as they notify the centroid state of the group of followers which tracks the path of the leader continuously. Dongbin et al., in ref. [6], have proposed another approach of formation control for nonholonomic mobile robots based on decentralized nonholonomic algorithms via second-order sliding mode control. The problem of formation control is resolved and maintains the desired separated distance and bearing angle between robots. Moreover, they archived its stability by using (L-φ)-based algorithm. In this regard, another contribution from Zhang et al., in ref. [7], has given the idea of formation control of NMR. First, the formation trajectory converted into a special tracking problem, and then, a neural network-based observer is applied to estimate the states of the leader vehicle.

In reality, the NMR is not equipped with sensors to measure velocity and position, due to the additional cost and weight on the structure of NMR. It is desirable to design a controller that make use of estimated states rather than measured ones. This requires the use of a suitable observer that can estimate the required states fast enough and with a degree of robustness against model perturbations or parametric uncertainties. Several researchers have contributed to the solution of this problem, thereby proposing various techniques and solutions [8, 9]. Asif et al., in ref. [8], have addressed the problem of estimating unknown states using a high-gain observer for WMR. The design of the controller is based on the adaptive output-feedback scheme for estimating the unknown states. Bowska et al., in ref. [10], suggested the observer for estimating the velocity. The speed estimation for nonholonomic portable robots associated with the environment is yet an open issue, especially when the robot needs to take later-differing speed direction. Finally, Astolfi et al., in ref. [9], suggested an observer for estimating velocity. They used neurodynamics observer in leaderless formation.

In this paper, we demonstrate a systematic development of a robust formation control scheme for NMRs. First, a robust stabilizing controller is designed using SMC technique that addresses the stabilization as well as tracking problem of the NMR. In the next step, we augment the SMC-based stabilizing controller with an integral terminal-based sliding mode control (ITSMC)-based formation controller that addresses the problem of formation control for multiple NMRs in a leader–follower scenario. This work can resemble in term of their dynamics with the past researches. However, the main difference lies in the designing of switching surface with the added term of integral. In a practical scenario, NMR may not be equipped with sensors to measure velocity and position, due to the additional cost and weight on the structure of NMR. To reduce this problem, the proposed control scheme is extended to output feedback by using high-gain observer. The novelty of this paper is to estimate those states which are unavailable to incorporate the effects of the kinematic model during

https://doi.org/10.1017/S026357471800142X Published online by Cambridge University Press

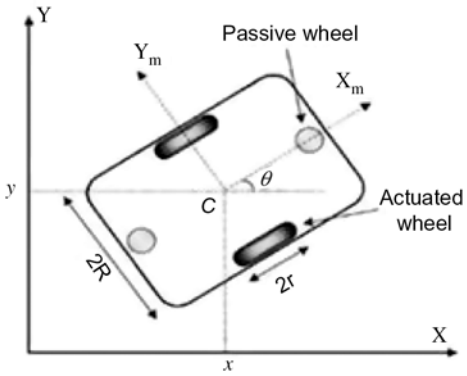

Fig. 1. Configuration of a unicycle robot.[11]

the design of nonlinear control to enhance robustness properties for better stability and accuracy. The complexity of control is reduced with the help of graph theory constraint. The closed-loop system performance analysis is carried out using Lyapunov stability methods. Convergence of system trajectories to the desired set while maintaining the special pattern is shown analytically as well as by simulation.

The remaining structure of the paper is organized as follows: Kinematic modeling of NMR is discussed in Section 2. The design of the desired control law for stabilization and tracking of NMR is established in Section 3. Section 4 discusses the formation model based on the graph theory constraint. It follows by the designing of the desired proposed control scheme. Section 5 presents the design of high-gain observer for estimating the position and velocity of NMR. Finally, concluding remarks and future recommendation are drawn in Section 6.

2. Problem Formulation

Consider a basic model of unicycle mobile robot with nonintegrable constraints, which can be seen in Fig. 1. The mathematical model of NMR is derived in Cartesian coordinate system (x, y).[2] The model is defined under the hypothesis of pure rolling and nonslipping surface as

$$\dot{p} = f(p, u) = \tau(p)u \tag{1}$$

where $p = [x_j, y_j, \theta_j]$ is the state vector, $u = [v_j, w_j]$ is the input vector and $\tau(p)$ is the rotation matrix expressed as

$$\tau(p) = \begin{bmatrix} cos\theta_j & 0 \\ sin\theta_j & 0 \\ 0 & 1 \end{bmatrix} \tag{2}$$

By substituting Eq. (2) in Eq. (1) equivalently, the kinematic model can be written as

$$\begin{aligned} \dot{x}_j &= v_j cos\theta_j \\ \dot{y}_j &= v_j sin\theta_j \\ \dot{\theta}_j &= w_j \end{aligned} \tag{3}$$

where (x_j, y_j) denotes the position of the center of mass of the robot and θ_j is the heading angle of the robot, respectively, v_j and w_j represent as linear and angular forward velocity of the robot. $(x_j(0), y_j(0), \theta_j(0))^T$ represent as the initial values of the parameters, respectively.

The possibility of modeling the kinematic equation of a wheeled mobile robot by so-called canonical chained form has been used in different papers.[3] For the purpose of designing a control scheme using SMC technique, it is desirable to convert the system (3) in a suitable canonical chained form such that desired control objectives can be achieved in a systematic manner. In this regard, we use

https://doi.org/10.1017/S026357471800142X Published online by Cambridge University Press

the input transformation approach as presented in ref. [1], to bring the system (3) in the following form:

$$\begin{cases} \dot{x}_0 = & u_0 \\ \dot{x}_1 = & x_2 u_0 \\ \dot{x}_2 = & u_1 - x_0 u_0 \\ \quad \vdots & \\ \dot{x}_n = & u_2 \end{cases}$$

For the system equation (1), by taking the following state and input transformation, the model converted as

$$x_0 = \theta_j, \quad x_1 = x_j sin\theta_j - y_j cos\theta_j$$
$$x_2 = x_j cos\theta_j + y_j sin\theta_j, u_0 = w_j, u_1 = v_j$$

one obtains

$$\begin{aligned} \dot{x}_0 &= u_0 \\ \dot{x}_1 &= x_2 u_0 \\ \dot{x}_2 &= u_1 - x_1 u_0 \\ y_1 &= x_0, \quad y_2 = x_1, \quad y_3 = x_2 \end{aligned} \tag{4}$$

The chained form in Eq. (4) has a strong underlying linear structure. The above system can be described in two subsystem as

$$\begin{aligned} \dot{X}_0 &= u_0 \\ \dot{X} &= AX + Bu_1 + D \end{aligned} \tag{5}$$

where $D = [d_1, d_2, d_3]$ is defined as the disturbance vector and X is defined as

$$X_0 = x_0$$
$$X = [x_1 \ \ x_2 \ \ \ldots \ \ x_n]^T$$

Assumption 1. *It is assumed that D can be upper bounded as shown below:*

$$|D(t)| \leq \varsigma$$

The matrix (A, B) in Eq. (3) can be defined as

$$A = \begin{bmatrix} 0 & u_0(t) & \ldots & 0 \\ 0 & 0 & \ddots & 0 \\ \ldots & \ldots & \ldots & u_0(t) \\ 0 & 0 & 0 & 0 \end{bmatrix}, \quad B = \begin{bmatrix} 0 \\ \vdots \\ 0 \\ 1 \end{bmatrix}$$

This clearly appears the second part of Eq. (5) becomes a single-input time-varying linear system when u_0 is taken as a function of time and no longer as a control variable. The selection of u_0 is very important to make sure the system is controllable in finite time. However, it can be uncontrollable due to the first part of Eq. (5) depends upon the selection of u_0. The second part of Eq. (5) is a state equation of linear system. We can apply the SMC to this system based on linear system theory.

The objectives of research in this paper are presented as follows:

- To design a stable point-to-point control law to stabilize the NMR at its equilibrium point.
- To design a tracking controller, which tracks the constant reference trajectory.
- To design an integral-based sliding mode formation control for NMR.
- To design an output-feedback formation control for estimating the states for better transient performance.

https://doi.org/10.1017/S026357471800142X Published online by Cambridge University Press

3. Robust Stabilization and Trajectory Tracking Control Design

3.1. Stabilization control

To achieve stabilization, we design a control law based on SMC. The proposed control scheme compiled in two steps. First, we determine a control u_1 which drive the system to its desired value in finite time. In second step, we choose a switching control u_0 which ensures system boundedness. Such a control law can be written as

$$u = u_0 + u_1 \tag{6}$$

The main goal of this paper is to drive the system states to its equilibrium point. For that, a switching function is defined for the system equation (5):

$$s = C * X \tag{7}$$

For sliding mode control, one of the most important things is to select a suitable matrix C for switching surface. The proposed control scheme is forcing the system states to slide along the surface and drive them to their desired states. For that, this following condition needs to be fulfilled:

$$S(t) = C = \begin{bmatrix} C_1 & C_2 \end{bmatrix} \begin{bmatrix} X_1 \\ X_2 \end{bmatrix} \tag{8}$$

Suppose the matrix C is so designed that the matrix CB is nonsingular. Therefore, the equivalent control law equation is defined as

$$u_1 = (CB)^{-1} CAX - D \tag{9}$$

In order to force the system dynamics to converge into the switching surface, impose the following sliding manifold that is defined as

$$\dot{s} = -a * sgn(s) \tag{10}$$

where $a > 0$.

Remark 1. This discontinuous function can be often used as a replacement of Eq. (10):

$$\dot{s} = \begin{cases} -asgns & |s| > \epsilon \\ -a\frac{s}{\epsilon} & |s| < \epsilon \end{cases}$$

The selection of the value of ϵ is important to overcome the problem of chattering. This will affect the accuracy of the controller. The equivalent control equation is defined as

$$u_1 = (CB)^{-1}(-CAX - a * sgn(s)) \tag{11}$$

For X_0 subsystem, we take the following control law as

$$u_0 = -k_0 \beta \tag{12}$$

where

$$\beta \begin{cases} sgn(X_0), & |X_0| > \varepsilon \\ X_0, & |X_0| \leq \varepsilon \end{cases}$$

$\varepsilon > 0$ is a small constant. It can clearly be observed that the control law u_0 is bounded by a constant $k_0\varepsilon$.

Lemma 1. *For any arbitrary condition $X_0(t_0) \neq 0$, where $t_0 \geq 0$, the equivalent solution $X_0(t)$ exists and globally regulated to zero.*[12]

https://doi.org/10.1017/S026357471800142X Published online by Cambridge University Press

Proof. Taking the Lyapunov function $V = \frac{1}{2}X_0^2$, a simple computation gives:

$$\dot{V} \begin{cases} -k_0 |X_0|, & |X_0| > \varepsilon \\ -k_0 X_0^2, & |X_0| \leq 0 \end{cases} \tag{13}$$

Refer from Lemma 1, we conclude that X_0 exists and $X_0 \to 0$ as $t \to \infty$.

The final control law equation is expressed as

$$u = (CB)^{-1}(CAX - a * sgn(s)) - k_0 X_0 \tag{14}$$

The switch function of the system is taken as

$$s = CX = \frac{x_1}{u_0} + x_2 \tag{15}$$

The final control inputs are

$$\begin{aligned} u_0 &= -k_0 x_0 \\ u_1 &= -x_2 - a * sgn(s) \end{aligned} \tag{16}$$

The closed-loop system is defined, after substituting Eq. (16) in Eq. (4):

$$\begin{aligned} \dot{x}_0 &= -k_0 x_0 \\ \dot{x}_1 &= -k_0 x_0 x_2 \\ \dot{x}_2 &= -x_2 - a * sgn(s) + k_0 x_0 x_1 \end{aligned} \tag{17}$$

3.1.1. Stability analysis. The closed loop system is stable under the proposed control scheme when considering the above sliding surface equation (10) s. Let a Lyapunov function be $V = \frac{1}{2}s^T s$. After taking the derivative, the equation becomes

$$\begin{aligned} \dot{V} &= s^T \dot{s} \\ \dot{V} &= sT(-a * sgn(s)) \\ \dot{V} &= -as^T sgn(s) \\ \dot{V} &= -a \|s\| \leq 0 \end{aligned} \tag{18}$$

For the stability analysis of the closed-loop system (17), we choose the Lyapunov function $V = \frac{1}{2}x_0^2 + \frac{1}{2}x_1^2 + \frac{1}{2}x_2^2$. Taking the derivative of the above equation, this new equation is stated as

$$\begin{aligned} \dot{V} &= x_0\dot{x}_0 + x_1\dot{x}_1 + x_2\dot{x}_2 \\ \dot{V} &= x_0[-k_0 x_0] + x_1[-k_0 x_0 x_2] + x_2[-x_2 - a * sgn(s) \\ &\quad + k_0 x_0 x_1] \\ &= -k_0 x_0^2 - x_2^2 - x_2 a * sgn(s) \\ &= -g_0 \|x\|^2 - x_2 a * sgn(s) \\ \dot{V} &< 0 \ \Omega \quad \|x_2\| \doteq 0 \end{aligned} \tag{19}$$

The above analysis is summarized in the following theorem:

Remark 2. For the system (4), under the control law (16), make the system stable at certain equilibrium point.

3.1.2. Implementation. This section presents the implementation of proposed control law established in subsection 3.1. The objective is to stabilize the single robot at the desired equilibrium point consider as origin. For the x_0 subsystem, we can choose the below control law:

$$u_0(x_0) \begin{cases} sign(x_0), & |x_0| > 0.5 \\ x_0, & |x_0| \leq 0.5 \end{cases}$$

https://doi.org/10.1017/S026357471800142X Published online by Cambridge University Press

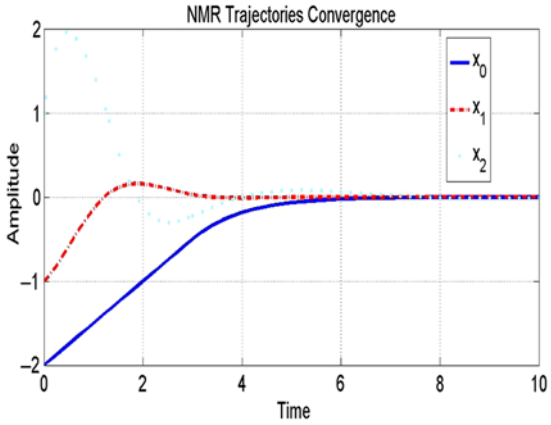

Fig. 2. NMR trajectories stabilize at origin.

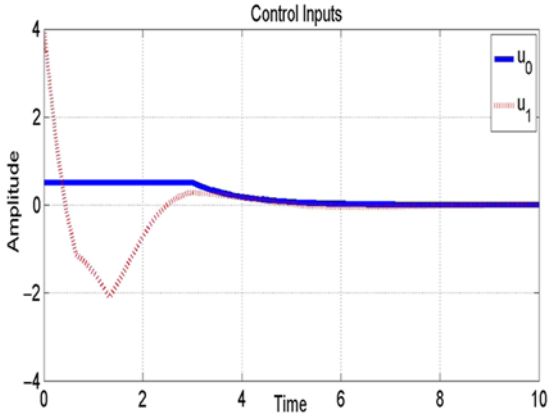

Fig. 3. Stabilzation control input.

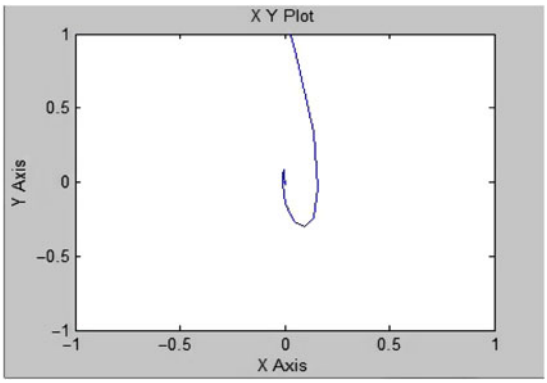

Fig. 4. NMR stabilzation in X-Y plane.

The performance results of the proposed controller have been shown through simulations in Figs. 2–6. The NMR initial state is being set as $p(0) = [2, 1, 1]^T$, whereas the controller parameters in Eq. (16) are defined as $k_0 = 5$, k_1, $k_2 = 6$, $a = 6$. State trajectories converge to zero over finite time are shown in Fig. 2. From which, it can be concluded that the system states are asymptotically regulated to zero. Figure 3 shows the graphical representation of the linear and angular velocities; the amplitude of the control input $u_0(w_j)$ is bounded by 0.5. Figure 4 shows the trajectory of the robot stabilized at the origin point. The system has proven to be globally uniformly stable (GUS). Figure 5 shows the trajectories in three-axis coordinates; it shows the trajectory stabilized at origin.

https://doi.org/10.1017/S026357471800142X Published online by Cambridge University Press

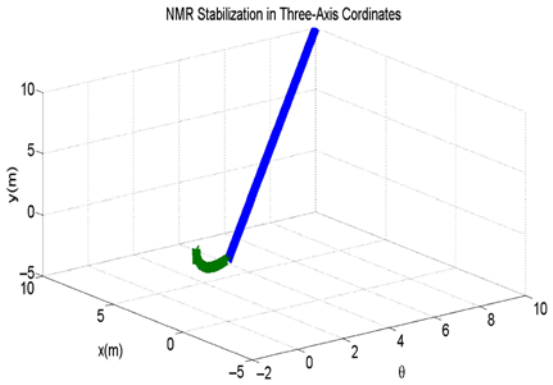

Fig. 5. NMR trajectories in three-axis plane.

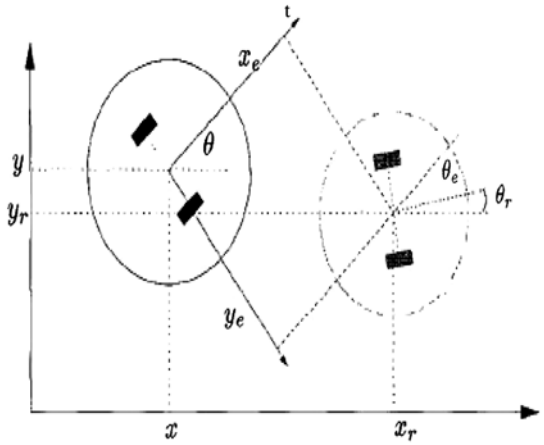

Fig. 6. Reference coordinate of NMR [6, 7].

3.2. Robust tracking control

In this subsection, the problem of tracking is addressed again for time-varying reference trajectories. In order to attain tracking of known time-varying trajectories, we also incorporate an additional control component to the control law to enable stabilization of an equilibrium that changes with respect to tracking signal. Starting with the mathematical equation of NMR, we demonstrate a systematic approach of robust tracking control scheme for NMR. The proposed control design objective is to follow the reference trajectory defined as follows:

$$\begin{aligned} \dot{x}_{jr} &= v_{jr} cos\theta_{jr} \\ \dot{y}_{jr} &= v_{jr} sin\theta_{jr} \\ \dot{\theta}_{jr} &= w_{jr} \end{aligned} \tag{20}$$

x_{jr}, y_{jr} are the position reference of the NMR, whereas θ_{jr} is the reference orientation angle. Proposed design of controller attempts to enable the robot to track itself to matchup the reference and stabilize at certain equilibrium point. For simplicity, we convert the system into an error model. Now, the global change of coordinates is introduced as

$$\begin{aligned} \dot{x} &= Ax + Bu + E(r) \\ e &= x - E(r) \end{aligned} \tag{21}$$

$E(r)$ is defined as reference trajectories. From Fig. 2, the error variable can be written as

$$\begin{bmatrix} e_{jx} \\ e_{jy} \\ e_{j\theta} \end{bmatrix} = \begin{bmatrix} cos\theta_j & sin\theta_j & 0 \\ -sin\theta_j & cos\theta_j & 0 \\ 0 & 0 & 1 \end{bmatrix} * \begin{bmatrix} x_j - x_{jr} \\ y_j - y_{jr} \\ \theta_j - \theta_{jr} \end{bmatrix} \tag{22}$$

https://doi.org/10.1017/S026357471800142X Published online by Cambridge University Press

By taking the derivative of Eq. (22), $\dot{e} = Ae + B[x_1 - r]u$. These new coordinates of the error model for a single NMR are described as

$$\begin{aligned} \dot{e}_{jx} &= w_j e_{jy} + v_j - v_{jr} cose_{j\theta} \\ \dot{e}_{jy} &= -w_j e_{jx} + v_{jr} sine_{j\theta} \\ \dot{e}_{j\theta} &= w_j - w_{jr} \end{aligned} \tag{23}$$

To simplify the problem, $e_{jx} = 0$ is selected as the first switching function. To find out the other switching function, we can use Lyapunov function that is expressed as $V = \frac{1}{2} e_{jy}^2$. By taking derivative, the equation can be written as

$$\begin{aligned} \dot{V} &= e_{jy} \dot{e}_{jy} \\ \dot{V} &= e_{jy}[-w_j e_{jx} + v_{jr} sine_{j\theta}] \\ \dot{V} &= -e_{jx} e_{jy} w_j - v_{jr} e_{jy} sin(atan(v_{jr} e_{jy})) \end{aligned} \tag{24}$$

where $e_{j\theta} = sin(atan(v_{jr} e_{jy}))$ chosen as switching function. $\dot{V} < 0$ if $v_{jr} e_{jy} sin(atan(v_{jr} e_{jy}) > 0$. Notice that, when e_{jx} converges to 0 and $e_{j\theta}$ converges to $atan(v_{jr} e_{jy})$, then this switching function can be obtained as

$$\begin{aligned} s_1 &= e_{jx} \\ s_2 &= e_{j\theta} + atan(v_{jr} e_{jy}) \end{aligned} \tag{25}$$

This approach not only forces the system states to reach the desired trajectory but also specifies the dynamic characteristics of the system. In order to reduce chattering which is caused by finite time delay and commutation, this switching function can be defined as

$$\dot{s} = -ksat(s) \tag{26}$$

The control equation can be derived from

$$\dot{s} = \begin{bmatrix} \dot{s}_1 \\ \dot{s}_2 \end{bmatrix} = \begin{bmatrix} \dot{e}_{jx} \\ \dot{e}_{j\theta} + \frac{\partial \beta}{\partial v_{jr}} \dot{v}_{jr} + \frac{\partial \beta}{\partial e_{jy}} (-e_{jx} w + v_{jr} sine_{j\theta}) \end{bmatrix} \tag{27}$$

where $\frac{\partial \beta}{\partial v_{jr}} = \frac{e_{jy}}{1+(v_{jr} e_{jy})}^2$ and $\frac{\partial \beta}{\partial e_{jy}} = \frac{v_{jr}}{1+(v_{jr} e_{jy})}^2$. The equation of the control law can be obtained with the above equation

$$\begin{aligned} v_j &= e_{jy} w_j + v_{jr} cose_{j\theta} + k_1 sat(s_1) \\ w_j &= w_{jr} + \frac{e_{jy}}{1 + (v_{jr} e_{jy})^2} \dot{v_{jr}} + \frac{v_{jr}}{1 + (v_{jr} e_{jy})^2} v_{jr} sine_{j\theta} \\ &\quad + k_2 sat(s_2) \end{aligned} \tag{28}$$

3.2.1. Stability analysis. This section discusses the stability analysis using Lyapunov function as $V = \frac{1}{2} s^T s$. By taking derivative, the equation can be expressed as

$$\begin{aligned} \dot{V} &= s^T[-ksat(s)] \\ \dot{V} &= -k \|s\| < 0 \end{aligned} \tag{29}$$

From the above analysis, it can be observed that $s(0) = 0$ and $\dot{V} \leq 0$, the system states converges on the sliding surface $s(t)$ and the trajectory tracking errors goes to zero in finite time.

3.2.2. Implementation. This section shows the implementation of the proposed SMC through simulation for constant reference trajectories. The NMR initial state is being set as $p(0) = [2, 1, 1]^T$, whereas the controller parameters in Eq. (28) are defined as $k_1 = -8$, $k_2 = -8$. The circular motion utilized in this simulation is considered as the reference trajectory. The linear velocity is undeviating, while the angular velocity is bounded at circular motion. Figure 7 shows the position error trajectories of NMR approaches toward zero. Figure 8 shows the control input which is continually varying as to matchup with the reference velocities. Figure 9 shows the trajectory tracking results of NMR for

https://doi.org/10.1017/S026357471800142X Published online by Cambridge University Press

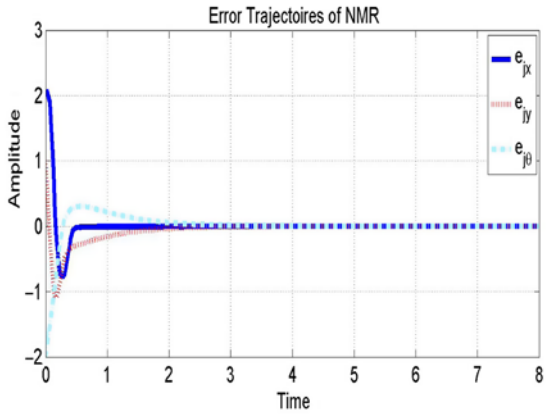

Fig. 7. NMR error trajectories convergence.

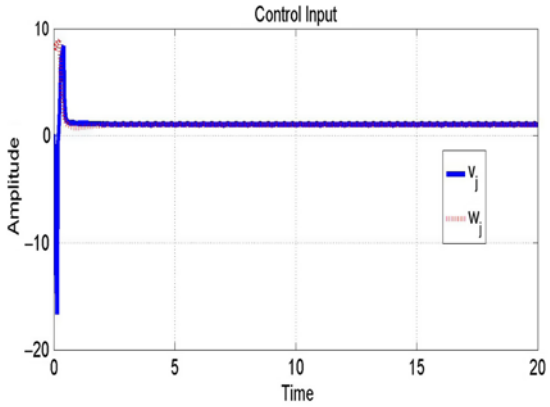

Fig. 8. Tracking control input.

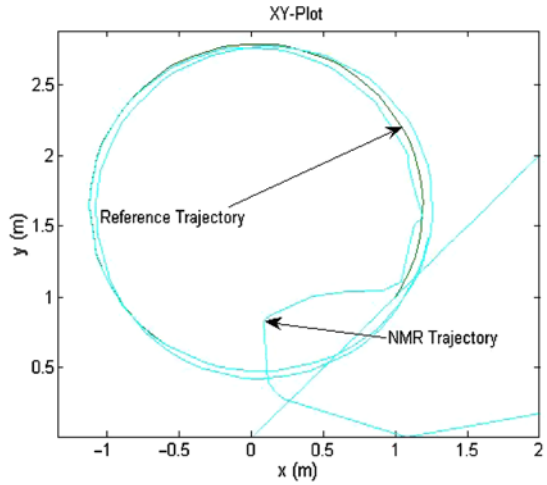

Fig. 9. NMR tracks reference trajectories in X-Y plane.

the circular reference. The robot follows the reference trajectory well in time. Figure 10 shows the sliding surface convergence. According to the simulation results for the circular motion, the motion of NMR remains in a stable position while it generates the position tracking error simultaneously. That is, the position of the robot converges to the desired trajectory. This demonstrates the efficacy of the sliding control algorithm hypothetically. Compare with the other solution mentioned in the

https://doi.org/10.1017/S026357471800142X Published online by Cambridge University Press

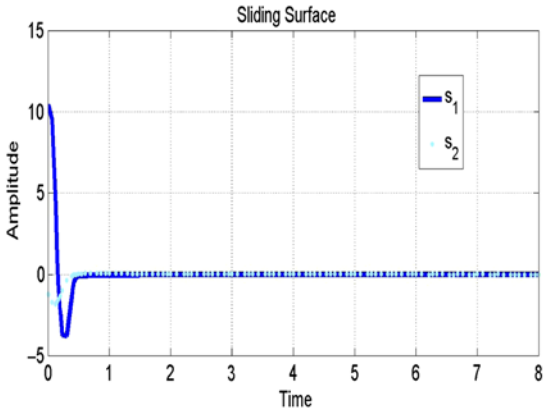

Fig. 10. Sliding surface.

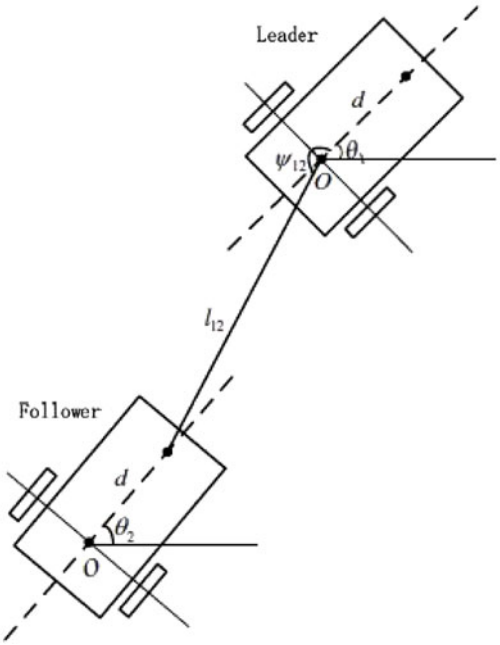

Fig. 11. L-φ formation model.

reference section, this control law remains in a certain bound, and the switch function varies with parameter according to the reference trajectory.

4. Formation Control

Consider two nonholonomic mobile robots shown in Fig. 11. Let the front robot be the leader and the other be the follower. The separation distance L_{oj} between the robots is measured from the origin of the two rear wheels of the leader robot to the front of the follower robot. The bearing angle φ_{oj} is measured from the heading angle of the leader robot to the distance line between the two robots. We assume that the offset d is large enough to avoid the collision among the follower robots.

4.1. Robust formation control

Stabilization and trajectory tracking of a single NMR with constant reference trajectories and its control based on sliding mode are discussed in earlier section. These results are verified analytically as well as by simulation. Once the stabilization and tracking are achieved, now we can consider the problem of formation control for a group of NMRs. The systematic model of NMR is reformulated as a formation model in a leader–follower scenario. A more robust control design technique is being

https://doi.org/10.1017/S026357471800142X Published online by Cambridge University Press

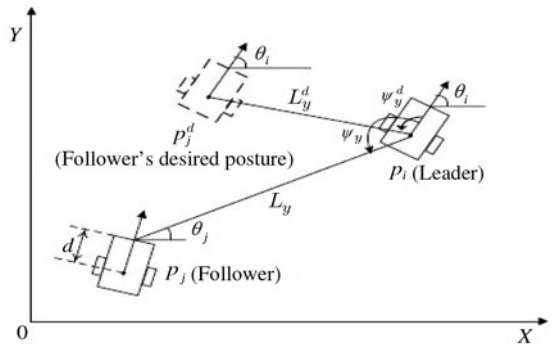

Fig. 12. Posture model of NMR.

developed based on the ITSMC. The proposed design of control ensures the tracking of the target point in the rigid structure while moving in a specific pattern. The zeroth robot is the virtual/leader robot and others are the followers. The problem is to design a control based on the neighbor states for each follower such that each robot comes into the formation while tracking the reference trajectory to reach desired target.

4.2. Graph theory

To address the communication limitations, which often cause major problems for each robot [5, 11], our proposed control law exploits following graph theory constraint. We represent n NMR as n vertices of a digraph $G(V, E)$. E is denoted as the edge on the vertices V. These edges are directed from the leader to the follower. The unidirectional symmetry protocol (directed graph) is used in this paper.

Node 0 represented the exogenous signal or leader robot which generates the reference signal for the followers. There will be a non-negative adjacency matrix. Adjacency matrix basically describes the flow of the instruction defined by the leader and map them in matrix form for the mathematical formulation. $A = A(G) = (a_{ij})$ is the nxn matrix, where $a_{ij} = 1$ if there is one edge $(j, i) \epsilon E$ otherwise $a_{ij} = 0$. The adjacency matrix a_{ij} for this problem is:

$$\begin{bmatrix} L \\ F_1 \\ F_2 \\ F_3 \\ F_4 \end{bmatrix} = \begin{bmatrix} 0\,1\,1\,0\,0 \\ 0\,0\,0\,1\,0 \\ 0\,0\,0\,0\,1 \\ 0\,0\,0\,0\,0 \\ 0\,0\,0\,0\,0 \end{bmatrix}$$

4.3. Leader–follower formation model

In this section, the model is reformulated as formation model using the full states of leader robot as shown in Fig. 12. Starting from the actual posture (initial condition) to the desired posture (the final position), let

$[x_0, y_0, \theta_0]$ be the actual posture of the leader
$[x_j, y_j, \theta_j]$ be the actual posture of the follower
$[x_j^d, y_j^d, \theta_j^d]$ be the desired posture of the follower

L_{0j} and ψ_{0j} are the actual separation and bearing among the robots, respectively. The desired posture q_j^d of NMR expresses as

$$\begin{aligned} q_j^d &= [x_j^d, y_j^d, \theta_j^d] \\ &= \begin{bmatrix} x_i - dcos\theta_j^d + L_{ij}^d cos(\varphi_{ij}^d + \theta_j^d) \\ x_i - dsin\theta_j^d + L_{ij}^d sin(\varphi_{ij}^d + \theta_j^d) \\ \theta_j^d \end{bmatrix} \end{aligned} \tag{30}$$

https://doi.org/10.1017/S026357471800142X Published online by Cambridge University Press

The actual posture of the follower NMR satisfies as

$$\begin{aligned} q_j &= [x_j, y_j, \theta_j] \\ &= \begin{bmatrix} x_i - dcos\theta_j + L_{ij}cos(\varphi_{ij} + \theta_j) \\ x_i - dsin\theta_j + L_{ij}sin(\varphi_{ij} + \theta_j) \\ \theta_j \end{bmatrix} \end{aligned} \tag{31}$$

Projection of the relative distance L_{ij} can be calculated as

$$L_{ij} = \sqrt{L_{0jx}^2 + L_{0jy}^2} \tag{32}$$

Relative distance can be written as Cartesian coordinates as

$$\begin{aligned} L_{ijx} &= x_0 - x_j - dcos\theta_j \\ L_{ijy} &= y_0 - y_j - dsin\theta_j \end{aligned}$$

By taking the derivative of the above equation, the dynamic is stated as

$$\begin{aligned} \dot{L}_{ijx} &= v_0 cos\theta_0 - v_j cos\theta_j + dw_j sin\theta_j \\ \dot{L}_{ijy} &= v_0 sin\theta_0 - v_j sin\theta_j + dw_j sin\theta_j \end{aligned}$$

Assumption 2. *The physical configuration of each robot is same and it is stabilized at certain equilibrium point.*

Assumption 3. *The desired angular velocity of the robot is bounded over finite time, and it is defined by the following equation:*

$-w_{max} \leq w_j \leq w_{max}$ where w_{max} is a positive constant

Assumption 4. *For each of the possible interaction topologies, $G_\sigma(t)$ at any followers, there exists a path from the leader the follower j. Moreover, the interaction between the robots is directed.*

Based on the above assumptions, we transformed the model equation (4) into the error model using relative distance and bearing angle. L_{oj}^d, φ_{oj}^d are defined as constants. Thus, one can obtain the error dynamics equation as

$$\begin{aligned} \dot{e}_{jx} &= v_0 cos\theta_{0j} + w_j e_{jy} - v_j - L_{0j}^d w_0 sin(\psi_{0j}^d + \theta_{0j}) \\ \dot{e}_{jy} &= v_0 sin\theta_{0j} - w_j e_{jy} - dw_j + L_{0j}^d w_0 cos(\psi_{0j}^d + \theta_{0j}) \\ \dot{e}_{j\theta} &= w_j^d - w_j \end{aligned} \tag{33}$$

where $\theta_{0j} = \theta_0 - \theta_j$. Due to characteristic of the error dynamic system equation (33), as per Assumption 4, the feedback controller can tackle this model. Another major problem is to control the orientation angle as the angle between robots will not be equal, while the formation is turning either side. For that problem, we must choose the desired posture angle as

$$\theta_j^d = (v_0 sin\theta_0 + L_{0j}^d cos(\psi_{0j}^d + \theta_{0j}) + 2k_2 e_{jy})/(e_{jx} + d)$$

4.4. Integral terminal sliding mode control design

In this section, we present the systematic approach of designing a control scheme. The key idea is to establish a sliding variable composed of tracking error and then drive these variables to zero via ITSMC. Let a singular continuous integral sliding surface be

$$s(t) = e(t) + k_1 \int_0^t e(\Gamma) d(\Gamma) \tag{34}$$

where k_1 is the positive coefficient and e is the formation tracking error which is defined as $e = [e_{jx}, e_{jy}]$.

https://doi.org/10.1017/S026357471800142X Published online by Cambridge University Press

Remark 3. The surface in Eq. (34) includes the integral action for tackling the position and orientation error trajectories and converges them to zero, keeps the system state close to the equilibrium point.

The derivative of Eq. (34) will give

$$\dot{s}(t) = \dot{e}(t) + k_1 e(t)$$

In order to keep the trajectory closed to the sliding surface s, the equivalent control can be derived when $\dot{s}(t) = 0$

$$\dot{s}(t) = \dot{e}(t) + k_1 e(t) = 0 \tag{35}$$

where $\dot{e}(t)$ defined as

$$\dot{e}(t) = F_1 + G_1 u_{equ} \tag{36}$$

Adding the *external locally Lipschitz continuous disturbance* η in prescribed system (33), we can rewrite the above Eq. (36) as

$$\dot{e}(t) = F_1 + G_1 u_{equ} + \eta \tag{37}$$

where F_1 and G_1 is formulated as

$$\begin{aligned} F_1(e_{jx}, e_{jy}, e_{j\theta}) &= \begin{bmatrix} v_0 cos\theta_{0j} & -L_{0j}^d w_0 sin(\varphi_{0j}^d + \theta_{0j}) \\ v_0 sin\theta_{0j} & L_{0j}^d w_0 cos(\varphi_{0j}^d + \theta_{0j}) \end{bmatrix} \\ \text{and } G_1(e_{jx}, e_{jy}, e_{j\theta}) &= \begin{bmatrix} -1 & y_{je} \\ 0 & -x_{je} - d \end{bmatrix} \end{aligned} \tag{38}$$

F_1 and G_1 are the velocity matrix of leader and follower, respectively. As the det of $(G_1(x_{je}, y_{je}\theta_{je})) = x_{je} + d \neq 0$, the inverse of G_1 always exists in this condition.

Substituting $\dot{e}$ into Eq. (36) yields the equivalent control law as

$$u_{equ} = -G_1^{-1}(F_1 + k_1 e(t) + \eta) \tag{39}$$

To assure the system states are on the sliding surface under the disturbance, the switching control law u_{swt} can be expressed as

$$\dot{u}_{swt} = -G_1^{-1}(-asat(s(t))) \tag{40}$$

where a is the switching gain parameter for compensating the system uncertainties and the turning effect of NMR. The $sat(.)$ is the saturation function used to eliminate chattering phenomenon. The $sat(.)$ function is given as

$$sat(s(t)) = \begin{cases} \frac{s(t)}{\varepsilon} & if \left|\frac{s_k(t)}{\varepsilon}\right| \leq 1 \\ sgn\left(\frac{s(t)}{\varepsilon}\right) & if \left|\frac{s_k(t)}{\varepsilon}\right| > 1 \end{cases} \quad k = 1, 2$$

where $sgn(.)$ is the standard signum function. The complete control law can be written as

$$\begin{aligned} u(t) &= u_{equ} + u_{swt} \\ u(t) &= -G_1^{-1}(F_1 + k_1 e(t) + \eta - u_{swt}) \end{aligned} \tag{41}$$

where $u = [v_j, w_j]$

The final equation of control input $[v_j, w_j]$ is

$$\begin{aligned} v_j = {} & v_0 cos\theta_{0j} - L_{0j}^d w_0 sin(\varphi_{0j}^d + \theta_{0j}) + k_1 e_{jx} + u_{swt} \\ & + \frac{e_{jy}}{e_{jx} + d}(v_0 sin\theta_{0j} - L_{0j}^d w_0 cos(\varphi_{0j}^d + \theta_{0j}) + k_1 e_{jy} \\ & + k_3 e_{j\theta} + u_{swt}) \\ w_{je} = {} & \frac{1}{x_{je} + d}(v_0 sin\theta_{0j} - L_{0j}^d w_0 cos(\varphi_{0j}^d + \theta_{0j}) + k_2 e_{jy} \\ & + k_3 e_{j\theta} + u_{swt}) \end{aligned} \tag{42}$$

https://doi.org/10.1017/S026357471800142X Published online by Cambridge University Press

The closed-loop system after substituting Eq. (42) in Eq. (33):

$$\begin{aligned} \dot{e_{jx}} &= -k_1 e_{jx} \\ \dot{e_{jy}} &= -w_j e_{jx} - k_2 e_{jy} - k_3 e_{j\theta} \\ \dot{e_{j\theta}} &= \frac{(k_2 e_{jy} - k_3 e_{j\theta})}{(e_{jx} + d)} \end{aligned} \tag{43}$$

Remark 4. The desired control law in Eq. (42) does not contain any singular term. It ensures the system error goes to zero and provides faster convergence of states to the equilibrium point near the sliding surface.

4.4.1. Stability analysis. Lyapunov analysis is used to carry out the stability of the proposed control law. Taking Lyapunov function as

$$V = \frac{1}{2} s^T(t) s(t) \tag{44}$$

Taking the derivative of the above equation yields

$$\begin{aligned} \dot{V} &= s^T(t)\dot{s}(t) \\ \dot{V} &= s^T(t)(F_1 + G_1 u(t) + k_1 e(t) + \eta) \end{aligned} \tag{45}$$

Substituting the equation of $u(t)$ in it, then the equation becomes

$$\begin{aligned} \dot{V} &= s^T(t)(u_{swt}) \\ \dot{V} &= s^T(t)(-asat(s(t))) \\ \dot{V} &= -as^T(t)sat(s(t)) \\ \dot{V} &= -a \, \|s(t)\| \leq 0 \end{aligned} \tag{46}$$

From Eq. (46), it can be observed that for $s(0) = 0$, $\dot{V} \leq 0$, it means the system converge to terminal sliding surface $s(t)$; therefore, the system force to remain in bound

These conditions satisfy the inside or outside boundary layers of the proposed controller

$$\begin{cases} -\frac{a}{\epsilon} \|s\|^2 < 0 & \|s\| \leq \epsilon \\ -asign \, \|s\|^{\frac{1}{2}} & \|s\| \geq \epsilon \end{cases}$$

Remark 5. The kinematic model in Eq. (3) satisfying all the Assumptions 2–4, the closed-loop system (33) will be bounded under the sliding mode control law (42).

4.4.2. Implementation. In this section, we demonstrate the performance of designed controller by use of five NMR (one leader and four followers), which can be seen in Fig. 13. We use leader vehicle as a reference. The controller gains and parameters used for simulation are selected as $k_1, k_2, k_3 = 8$, $a_1 = -0.11$, and the external disturbance (uncertainties) changes with respect to time described as $\eta = \left[\frac{0.01}{2+t} \ \frac{0.01}{1+\frac{1}{t+1}}\right]$. From Fig. 13, it shows that F_1 and F_2 follow the leader L, F_4 follows F_2 and F_3 follows F_1. It can be seen clearly F_2 will be leader for F_4 and F_1 will be leader for F_3. The offset distance between the followers is $d = 0.6$ cm. The reference trajectory can be obtained with the help of the following equation:

$$v_i = sin(0.005\pi) + 1, \quad w_i = 0.1 sin(0.02\pi) \tag{47}$$

The desired separation-bearing are set as $z_1 = [L_{01}^d, \varphi_{01}^d] = (1, 240)$, $z_2 = [L_{02}^d, \varphi_{02}^d] = (2, 480)$, $z_3 = [L_{13}^d, \varphi_{13}^d] = (1, 240)$ and $z_4 = [L_{24}^d, \varphi_{24}^d] = (2, 480)$. The initial position of each robot is set as $L = (0.3, 05, 100)$, $F_1 = (2.5666, -1.7, 90)$, $F_2 = (1.5, 3, 0)$, $F_3 = (-0.5331, -2.5026, 45)$ and $F_4 = (-1.1356, 1.1, 30)$.

The desired trajectory assures the Assumption 4, and for reducing the difficulty, we assume the communication topology G to be fixed using the proposed control scheme extracted from Remark. The simulation results are shown in Figs. 14–20. Figures 14–17 show the convergence of tracking error of all the four followers toward zero. The errors converge to zero quickly less than 2 s under

https://doi.org/10.1017/S026357471800142X Published online by Cambridge University Press

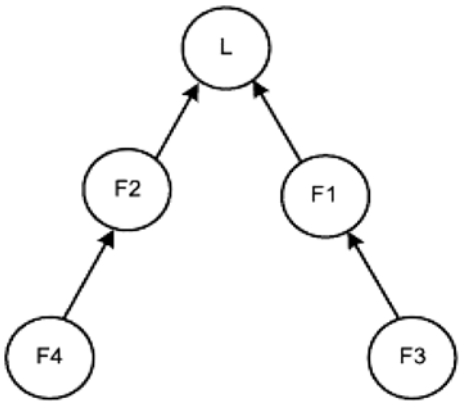

Fig. 13. Geometrical V-shaped formation.

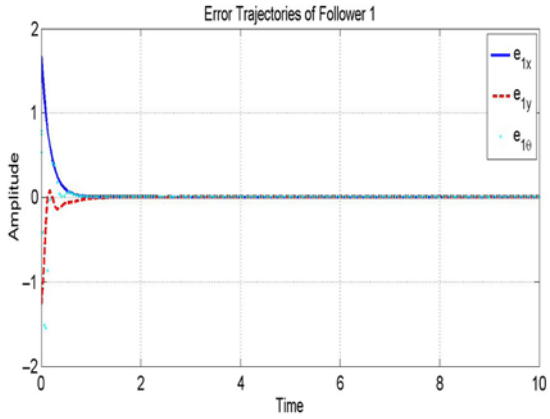

Fig. 14. Follower 1 error trajectories convergence.

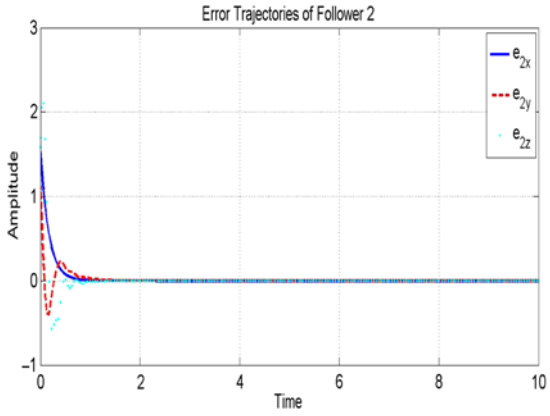

Fig. 15. Follower 2 error trajectories convergence.

the formation control strategy. As we compare with the existing result, it converges faster than the previous algorithms. Figure 18 shows the angular and linear velocities required for formation control. It shows the control input which is continually varying as to matchup with the reference velocities in the presence of disturbance. Figure 19 shows formation trajectories using ITSMC. Figure 20 shows the sliding surface convergence.

4.4.3. Comparison. The four follower's robot tracks the leader with better accuracy compared to other researches mentioned in the reference section. It is much better and more robust while maintaining the desired separation and orientation. It can be seen that the robots form a desired fixed

https://doi.org/10.1017/S026357471800142X Published online by Cambridge University Press

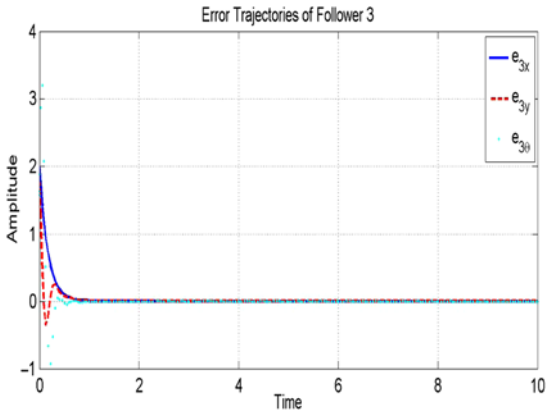

Fig. 16. Follower 3 error trajectories convergence.

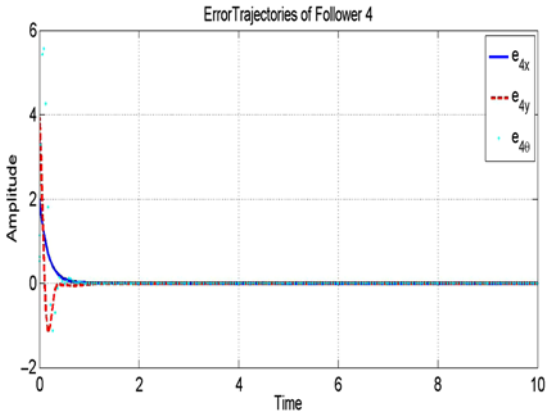

Fig. 17. Follower 4 error trajectories convergence.

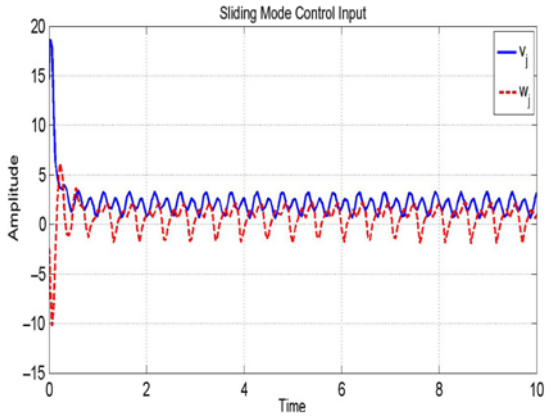

Fig. 18. Intergral sliding based control input.

triangle structure in their motion after a finite time, which concludes that the formation is well established and the system is stable under the proposed control scheme. It also can be an observer that the desired control provides better stability against the time-varying uncertainties.

5. Robust Output-Feedback Control Design

In reality, the NMR is not equipped with the sensors to measure velocity and position, due to the additional circuitry for velocity measurement. For this, it required additional cost and weight on the structure of NMR. It is desirable to design a controller that makes use of estimated states rather than

https://doi.org/10.1017/S026357471800142X Published online by Cambridge University Press

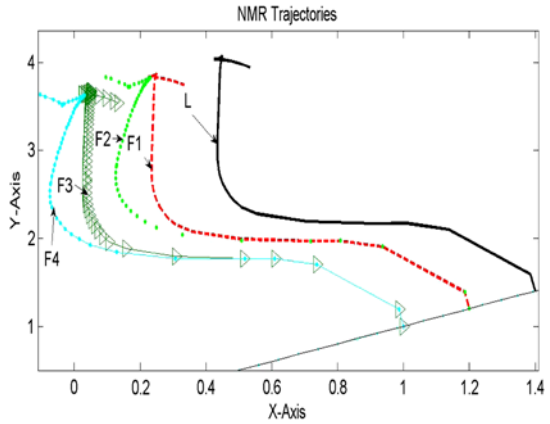

Fig. 19. NMR formation trajectories in X-Y plane.

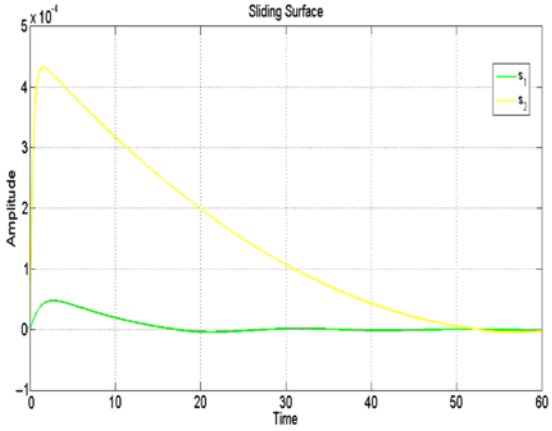

Fig. 20. Sliding surface trajectories.

measured ones. Therefore, an output-feedback controller is used to estimate the position and velocity of the NMR. It has been observed that a high-gain observer can recover the transient properties of ITSMC in the presence of disturbances. The most important part is to incorporate the effects of the kinematic model during the design of nonlinear control to enhance robustness properties for better stability and accuracy. To design a high-gain observer, the error model equation (33) can be transformed into an observer form as

$$\begin{aligned}
\hat{\dot{e}}_{jx} &= v_0 cos\theta_{0j} + w_j \hat{e}_{jy} - v_j - L_{0j}^d w_0 sin(\psi_{0j}^d + \theta_{0j}) \\
&\quad + h_1(e_{jx} - \hat{e}_{jx}) \\
\hat{\dot{e}}_{jy} &= v_0 sin\theta_{0j} - w_j \hat{e_{jx}} - dw_j + L_{0j}^d w_0 cos(\psi_{0j}^d + \theta_{0j}) \\
&\quad + h_2(e_{jy} - \hat{e}_{jy}) \\
\hat{\dot{e}}_{j\theta} &= w_j^d - w_j + h_3(e_{j\theta} - \hat{e}_{j\theta})
\end{aligned} \tag{48}$$

The equation of the desired orientation angle can be transformed as

$$\begin{aligned}
\theta_j^d = (v_0 sin\theta_0 + L_{0j}^d cos(\psi_{0j}^d + \theta_{0j}) + 2k_2 \hat{e}_{jy} + u_{12}) \\
(\hat{e}_{jx} + d)
\end{aligned}$$

The high-gain observer-based error model can be described as

$$\begin{aligned}
\tilde{e}_{jx} &= e_{jx} - \hat{e}_{jx} \\
\tilde{e}_{jy} &= e_{jy} - \hat{e}_{jy} \\
\tilde{e}_{j\theta} &= e_{j\theta} - \hat{e}_{j\theta}
\end{aligned} \tag{49}$$

https://doi.org/10.1017/S026357471800142X Published online by Cambridge University Press

By *taking the derivative* of Eq. (49) and substituting Eqs. (33) and (48) in Eq. (49)

$$\begin{aligned}
\dot{\tilde{e}}_{jx} &= v_o cos\theta_{0j} + w_j e_{jy} - v_j - L_{0j}^d w_0 sin(\psi_{0j}^d + \theta_{0j}) \\
&\quad - v_0 cos\theta_{0j} - w_j \hat{e}_{jy} + v_j + L_{0j}^d w_0 sin(\psi_{0j}^d + \theta_{0j}) \\
&\quad - h(e_{jx} - \hat{e}_{jx}) \\
\dot{\tilde{e}}_{jx} &= w_j \tilde{e}_{jy} - h_1 \tilde{e}_{jx} \\
\dot{\tilde{e}}_{jy} &= -w_j \tilde{e}_{jx} - h_2 \tilde{e}_{jy} \\
\dot{\tilde{e}}_{j\theta} &= \frac{1}{e_{jx}+d}(k_2 e_{jy} - k_3 e_{j\theta}) - \frac{1}{\hat{e}_{jx}+d}(k_2 \hat{e}_{jy} - k_3 \hat{e}_{j\theta}) \\
&\quad - h_3 \tilde{e}_{j\theta}
\end{aligned}$$

Let $a = \frac{1}{x_{je}+d}$, then the system becomes

$$\begin{aligned}
\dot{\tilde{e}}_{jx} &= w_j \tilde{e}_{jy} - h_1 \tilde{e}_{jx} \\
\dot{\tilde{e}}_{jy} &= -w_j \tilde{e}_{jx} - h_2 \tilde{e}_{jy} \\
\dot{\tilde{e}}_{j\theta} &= a(k_2 e_{jy} - k_3 e_{j\theta}) - \hat{a}(k_2 \hat{e}_{jy} - k_3 \hat{e}_{j\theta}) - h_3 \tilde{e}_{j\theta} \\
\dot{\tilde{e}}_{j\theta} &= k_2(a e_{jy} - \hat{a}\hat{e}_{jy}) - k_3(a e_{j\theta} - \hat{a}\hat{e}_{j\theta}) - h_3 \tilde{e}_{j\theta} \\
\dot{\tilde{e}}_{j\theta} &= k_2 \tilde{a} \tilde{e}_{jy} - k_3 \tilde{a} \tilde{e}_{j\theta} - h_3 \tilde{e}_{j\theta} \\
\dot{\tilde{e}}_{j\theta} &= \frac{1}{\tilde{e}_{jx}+d}(k_2 \tilde{e}_{jy} - k_3 \tilde{e}_{j\theta}) - h_3 \tilde{e}_{j\theta}
\end{aligned} \tag{50}$$

The kinematic control equation (42) can be written as

$$\begin{aligned}
v_j &= v_0 cos\theta_{0j} - L_{0j}^d w_0 sin(\varphi_{0j}^d + \theta_{0j}) + k_1 \tilde{e}_{jx} + u_{11} \\
&\quad + \frac{\tilde{e}_{jy}}{\tilde{e}_{jx}+d} * (v_0 sin\theta_{0j} - L_{0j}^d w_0 cos(\varphi_{0j}^d + \theta_{0j}) \\
&\quad + k_1 \tilde{e}_{jy} + k_1 \tilde{e}_{j\theta} + u_{12}) \\
w_{je} &= \frac{1}{\tilde{e}_{jx}+d}(v_o sin\theta_{0j} - L_{0j}^d w_0 cos(\varphi_{0j}^d + \theta_{0j}) \\
&\quad + k_2 \tilde{e}_{jy} + k_3 \tilde{e}_{j\theta} + u_{12})
\end{aligned} \tag{51}$$

5.1. Stability analysis

To prove the stability of the desired system in Eq. (50) we can use an energy function (Lyapunove function) to carry out the perfromace of the design controller.

Consider a Lyapunov function as

$$V(t) = 1/2 * (\tilde{e}_{jx}^2 + \tilde{e}_{jy}^2) + (\tilde{e}_{jx} + d)\frac{k_3 \tilde{e}_{j\theta}^2}{2k_2} \tag{52}$$

By taking derivative, the equation can be written as

$$\dot{V}(t) = \tilde{e}_{jx}\dot{\tilde{e}}_{jx} + \tilde{e}_{jy}\dot{\tilde{e}}_{jy} + (\tilde{e}_{jx} + d)\frac{k_3 \tilde{e}_{j\theta}\dot{\tilde{e}}_{j\theta}}{k_2} \tag{53}$$

$$\begin{aligned}
\dot{V}(t) = &\ \tilde{e}_{jx}(w_j \tilde{e}_{jy} - h_1 \tilde{e}_{jx}) + \tilde{e}_{jy}(-w_j \tilde{e}_{jx} - h_2 \tilde{e}_{jy}) \\
&+ \tilde{e}_{j\theta}(\tilde{e}_{jx} + d)\frac{k_3 \tilde{e}_{j\theta}}{k_2}\left(\frac{(k_2 \tilde{e_{jy}} - k_3 \tilde{e}_{j\theta})}{(\tilde{e}_{jx}+d)} - h_3 \tilde{e}_{j\theta}\right)
\end{aligned}$$

https://doi.org/10.1017/S026357471800142X Published online by Cambridge University Press

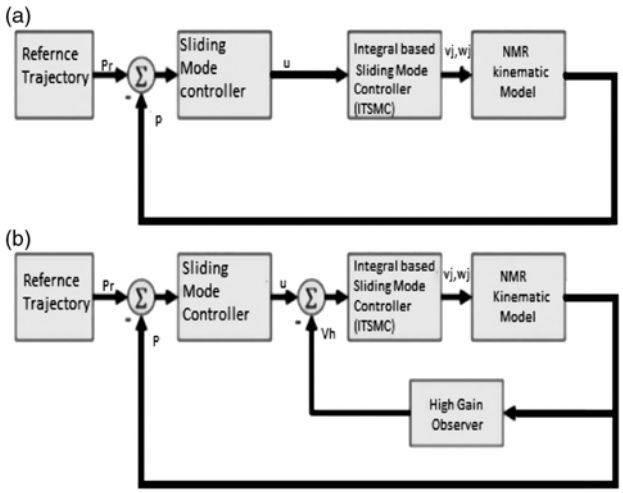

Fig. 21. Comparison between state-feedback and output-feedback system.[8]

$$\dot{V}(t) = -h_1\tilde{e}_{jx}^2 - h_2\tilde{e}_{jy}^2 + k_3\tilde{e}_{j\theta}\tilde{e}_{jy} - \frac{k_3\tilde{e}_{j\theta}^2}{k_2} - \frac{h_3k_3}{k_2}\tilde{e}_{j\theta}\tilde{e}_{jx} - \frac{h_3k_3}{k_2}\tilde{e}_{j\theta}^2 * d$$

$$\dot{V}_0(t) = -h_1e_{jx}^2 - h_2e_{jy}^2 - k_3e_{j\theta}^2 - \frac{h_3k_3}{k_2}\tilde{e}_{j\theta}^2 \leq -g_0\|x\|^2$$

$$\dot{V}(t) = -g_0\|x\|^2 + k_3\tilde{e}_{jy}\tilde{e}_{j\theta} - h_3\tilde{e}_{j\theta}^2\tilde{e}_{jx}$$

To prove the system stabilty, we assume k_3 and the conversion of the above equation into matrix form is as follows:

$$\dot{V}(t) = -\begin{bmatrix}\tilde{e}_{jx} & \tilde{e}_{jy}\end{bmatrix}\begin{bmatrix}\beta\tilde{e}_{j\theta} & 0\\ 0 & -\alpha\tilde{e}_{j\theta}\end{bmatrix}\quad\begin{bmatrix}\tilde{e}_{jx}\\ \tilde{e}_{jy}\end{bmatrix} < 0$$

$$\text{let } \Delta = \begin{bmatrix}\beta\tilde{e}_{j\theta} & 0\\ 0 & -\alpha\tilde{e}_{j\theta}\end{bmatrix}$$

V is the positive function. For ensuring system stability, $\dot{V}(t)$ should be negative definite, under the assumption that $\alpha < 0$ and $\beta, d > 0$. If the $\det(\Delta) > 0$ (positive definite), the system will be stable. Taking the derivative, the equation becomes

$$\Delta = \begin{bmatrix}\beta\tilde{e}_{j\theta} & 0\\ 0 & \alpha\tilde{e}_{jx}\end{bmatrix}$$

$$\det(\Delta) = \beta\tilde{e}_{j\theta} * -\alpha\tilde{e}_{j\theta}$$

$$\det(\Delta) = -\beta\alpha\tilde{e}_{j\theta}^2$$

$$\dot{V(t)} \leq 0 \text{ for } \det(\Delta) > 0\ \ \Omega\ \ \alpha < 0$$

The Lyapunov analysis shows that the proposed control scheme addresses in this section eliminates the tracking error, under the condition that some gains are positive constants.

5.1.1. Implementation. This section provides the simulation results to show the robustness of the desired proposed approach. A descriptive comparison between the state-feedback and output-feedback control can be seen in Fig. 21. It can be concluded that from Fig. 21, the desired proposed approach removes the inner-feedback loop, and the control input velocities are estimated using the high-gain observer. The simulation is illustrated on the same reference sine trajectory, which is used earlier in Section IV. The NMR gains and parameter use for simulation in the desired control law selected as $k_3 = -10$, $h_i > 0$, $i \epsilon [1, 3]$ are set as 6.

https://doi.org/10.1017/S026357471800142X Published online by Cambridge University Press

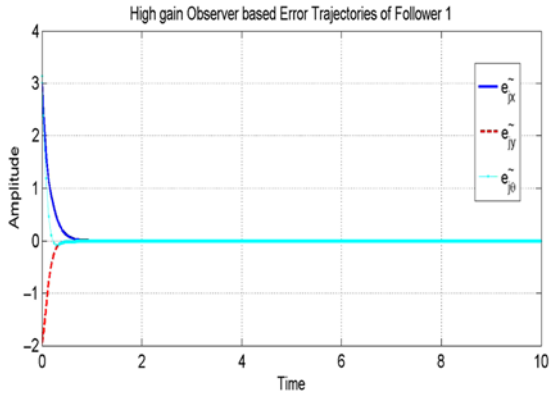

Fig. 22. Follower 1 error trajectories convergence.

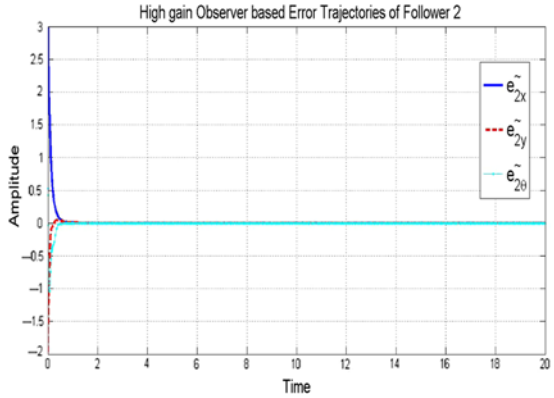

Fig. 23. Follower 2 error trajectories convergence.

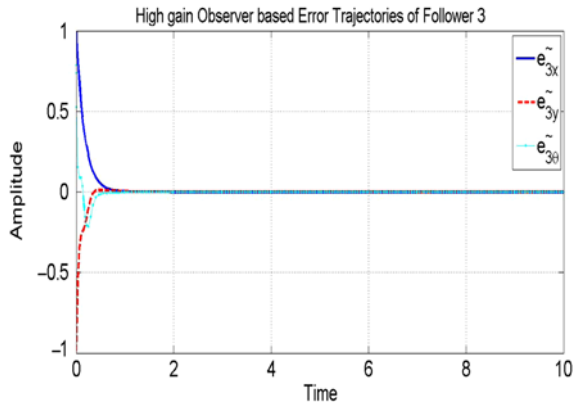

Fig. 24. Follower 3 error trajectories convergence.

The sine trajectory is defined with the following equations, which can be stated as

$$v_i = sin(0.005\pi) + 1, \quad w_i = 0.1sin(0.02\pi) \tag{54}$$

The desired separation-bearing are set as $z_1 = [L_{01}^d, \varphi_{01}^d] = (1, 240)$, $z_2 = [L_{02}^d, \varphi_{02}^d] = (2, 480)$, $z_3 = [L_{13}^d, \varphi_{13}^d] = (1, 240)$ and $z_4 = [L_{24}^d, \varphi_{24}^d] = (2, 480)$ with the initial position of each robot is set as $L = (0.3, 05, 100)$, $F_1 = (2.5666, -1.7, 90)$, $F_2 = (1.5, 3, 0)$, $F_3 = (-0.5331, -2.5026, 45)$ and $F_4 = (-1.1356, 1.1, 30)$.

Figures 22–25 describe the position tracking trajectories of the followers, which are approached to zero in finite time of <1.2 s. Figure 26 presents the comparison of linear and angular velocities of

https://doi.org/10.1017/S026357471800142X Published online by Cambridge University Press

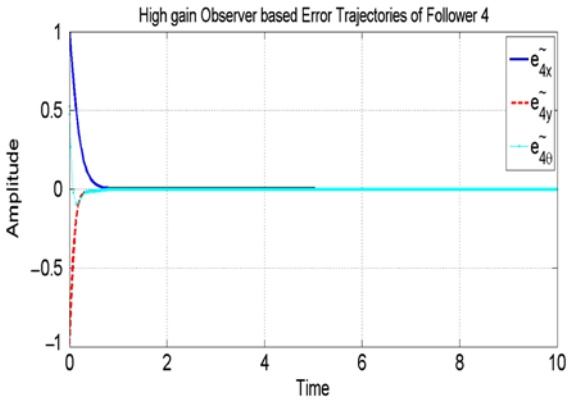

Fig. 25. Follower 4 error trajectories convergence.

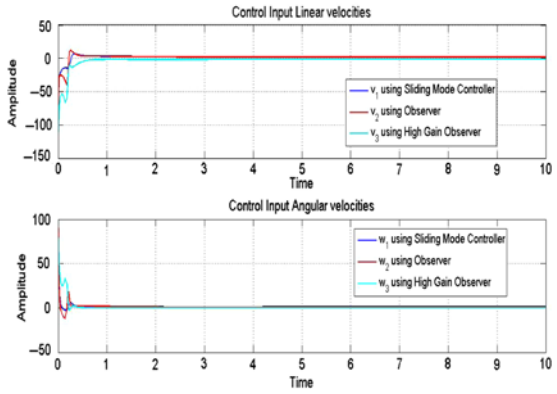

Fig. 26. High gain observer based control input comparision.

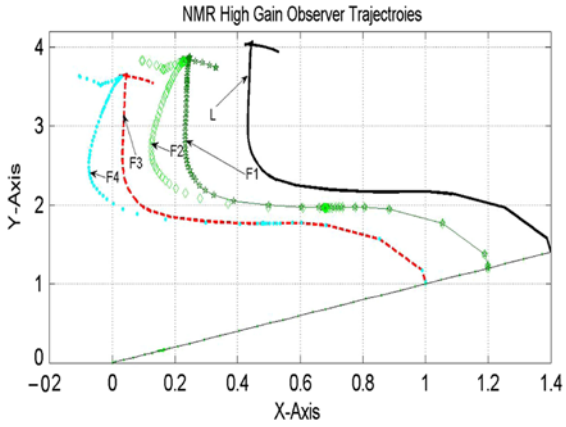

Fig. 27. NMR trajectories in X-Y plane.

state-feedback and the output-feedback control. It can be seen that there are less perturbations in the output feedback estimated control input, and it recovers the performance of state-feedback controller in finite time. Figure 27 demonstrates the tracking performance of NMR with an output-feedback controller; It can conclude the formation is well stable and robust compared to existing techniques. Figure 28 shows the comparison of state-feedback control (ITSMC) with output-feedback control High Gain Observer (HGO). It clearly shows the output-feedback control recover the performance of state-feedback control in the presence of uncertainties, in the region of interest.

https://doi.org/10.1017/S026357471800142X Published online by Cambridge University Press

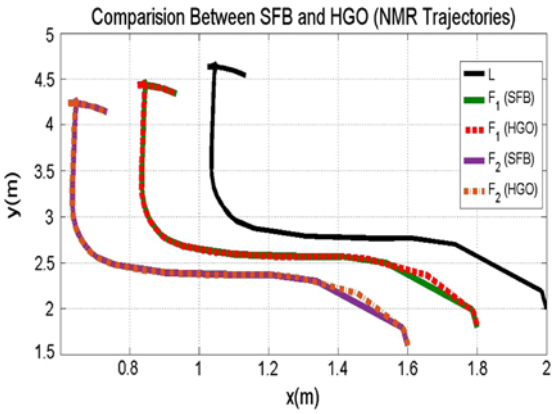

Fig. 28. Comparison between SFB and HGO.

6. Conclusion

In this paper, we present a systematic approach to design a robust formation control for NMRs. We use the properties of the system structure together with the SMC basic theory and augmented with the ITSMC to design a suitable formation control. The mathematical model exploits and reformulated into the formation model with the help of graph theory constraint. The proposed control scheme provides for desired robustness properties in the presence of the parametric variations, in the region of interest. The geometrical V-shaped formation has been simulated, and successive results are shown. The state-feedback control scheme is extended to output feedback by incorporating a high-gain observer. With the help of Lyapunov analysis and appropriate simulations, it is shown that the proposed output-feedback control scheme achieves the required control objectives and provides for the desired performance in the presence of parametric variations.

7. Future Recommendation

In this paper for simplicity, the communication topology is assumed to be fixed and connected. Hence, in the future, the first recommendation is to consider the formation control with time-varying delays. Another recommendation is to add an obstacle avoidance algorithm in the proposed control scheme with the extended high-gain observer for achieving robustness in the transient performance. This will definitely improve the practicality of NMR navigation. The last recommendation for extension is to make a decoupled reconfigurable formation control using digraph, which will enhance the consistency of the NMR formation.

References

1. F. Gao and Y. Shang,"Global state-feedback stabilization for a class of uncertain nonholonomic systems with partial inputs saturation," *WSEAS Trans. Circuits Syst.* **14**(1), 229–235 (2015).
2. J. H. Lee, C. Lin, H. Lim and J. M. Lee, "Sliding mode control for trajectory tracking of mobile robot in the RFID sensor space," *Int. J. Control Autom. Syst.* **7**(3), 429–435 (2009).
3. E. Lefeber, J. Jakabiuk and H. Nejimenjer, "Observer based kinematic tracking controller for a unicycle-type mobile robots," *IEEE Int. Conf. Rob. Autom.* **64**(5), 2084–2089 (2001).
4. Z. Peng, G. Weng and A. Rahmani, "Leaderfollower formation control of nonholonomic mobile robots based on a bioinspired neurodynamic based approach," *Rob. Auton. Syst.* **61**(5), 988–996 (2013).
5. L. Dong, Y. Chen and X. Qu, "Formation control strategy for nonholonomic intelligent vehicles based on virtual structure and consensus approach," *Procedia Eng.* **137**(8), 415–424 (2016).
6. S. Dongbin, S. Zhendong and Q. Yupeng, "Second-Order Sliding Mode Control for Nonholonomic Mobile Robots Formation," *Proceedings of the 30th Chinese Control Conference*, Yantai, China, (2011) pp. 4860–4864.
7. C. Zhang, T. Sun and Y. Pan, "Neural network observer-based finite-time formation control of mobile robots," *Math. Prob. Eng.* **2014**, 267307 (2011).
8. M. Asif, A. Y. Memon and M. J. Khan, "Output feedback control for trajectory tracking of wheeled mobile robot," *Intell. Autom. Soft Comput.* **22**(1), 75–87 (2015).
9. A. Astolfi, R. Ortega and A. Venkatraman, "A globally exponentially convergent immersion and invariance speed observer for mechanical systems with non-holonomic constraints," *IEEE Trans. Indus. Electron.* **58**(01), 182–189 (2016).

https://doi.org/10.1017/S026357471800142X Published online by Cambridge University Press

10. J. Bowska, "A velocity observer design for tracking task-based motions of unicycle type mobile robots," *Commun. Nonlinear Sci. Numer. Simul.* **16**, 2301–2307 (2011).
11. K.-C. Cao, "Formation Control of Multiple Nonholonomic Mobile Robots Based on Cascade Design," *Joint 48th IEEE Conference on Decision and Control and 28th Chinese Control Conference Shanghai*, P.R. China (2009).
12. B. M. Yousuf and A. Y. Memon, "Robust Trajectory Tracking Control Design for Nonholonomic Mobile Robot (NMR)," *Proceedings of the 3rd Australia New Zeland Control COnference (ANZCC)*, Melbourne, Australia (2018).

https://doi.org/10.1017/S026357471800142X Published online by Cambridge University Press